Journal of Engineering Physics and Thermophysics, Vol. 76, No. 6, 2003

CONTROL OF THE PARAMETERS OF AN EXHAUST JET BY INCREASING THE EDDY VISCOSITY AT THE NOZZLE EDGE

A. N. Kucherov

UDC 533.6

We studied the possibility of changing the parameters of the exhaust wake in the far field of the jet behind a large passenger aircraft (aerobus) by increasing the coefficient of eddy viscosity at the edge of the nozzle of a double-flow engine with a high double-flow ratio (>10) without mixing with the aid of artificial turbulizers created in the outer and inner ducts. Within the model of turbulence with one differential equation for the coefficient of viscosity, we obtained numerical solutions for velocity, temperature, concentrations of vapor and condensate, and the coefficient of viscosity for different variants which disclose the essence of a physico-mathematical model of the phenomenon and predict possible changes of the parameters of the exhaust jet with artificial increase of viscosity in the initial section and the jet volume.

Introduction. Ecological problems related to control and monitoring of harmful exhausts of aviation transport in the atmosphere require a thorough investigation of the gasdynamic, thermodynamic, physico-chemical, and optical parameters of the exhaust wake [1–4]. We consider the possibility of control over the parameters of the exhaust jet by increasing the degree of turbulization at the edge of the engine nozzle. We study a typical exhaust jet from a double-flow engine with a high double-flow ratio (>10) without mixing of flows of the inner hot and outer cold ducts. For description of the process of turbulent diffusion we select a one-parameter model of turbulence where the coefficient of turbulent kinematic viscosity ν is calculated by one differential equation of diffusion with one parameter, α_ν [5–11]. It is known that changes of the initial profiles of temperature, velocity, and concentration of any component affect the distributions of parameters in the near field (~10 radii of the nozzle) of a turbulent jet [12]. In ecological problems, the jet is considered at a distance of tens of kilometers up to complete attenuation which passes through four stages: jet, vortical, dispersion, and diffusion [2, 4]. As a rule, isobaric jets are considered and uniform (constant) transverse distributions of velocity, temperature, and other parameters are specified at the edge of the exhaust nozzle [1, 2]. In this case, it is indirectly assumed that in the far field (≥100 radii of the nozzle) these details are "forgotten." However, in [13] it is shown that relatively small changes in mean temperature (~10 K) or vapor concentration in the initial cross section can lead to 100% changes of the characteristics in the far field. We studied the effect of nonisobaricity [14] and initial transverse distributions of velocity, temperature, and concentration of vapor [15, 16] on the parameters of the exhaust jet in the cross section, where condensate merges on the axis, and on the far field. It is shown that small deviations of the inefficiency (nonisothermicity) ratio (20%) can lead to substantial changes in the characteristics of the far field [14]. The assignment of transverse distributions of temperature and velocity in the initial cross section, which are more close to real than uniform distributions, can result in a situation where in one case the condensation wake forms and in another it does not [15]. In the present paper, we study the effect of enhancement of flow turbulence on the parameters of the jet. In order to distinguish the effect of enhancement of the coefficient of eddy viscosity, we assume, not restricting the generality, that the jet is isobaric and the flow in the initial cross section is uniform in both ducts.

Problem Formulation. The isobaric axisymmetric jet is described by the following system:

$$p \approx p_\infty, \quad \rho = \frac{p_\infty m}{RT}, \tag{1}$$

Prof. N. E. Zhukovskii Central Aerohydrodynamic Institute, 1 Zhukovskii Str., Zhukovskii, Moscow Region, 140180, Russia; email: ank@aerocentr.msk.su. Translated from Inzhenerno-Fizicheskii Zhurnal, Vol. 76, No. 6, pp. 29–37, November–December, 2003. Original article submitted March 18, 2003.

1062-0125/03/7606-1227$25.00

$$\rho u\frac{\partial \nu}{\partial x}+\rho w\frac{\partial \nu}{\partial r}=\frac{2}{r}\frac{\partial}{\partial r}\left\{r\mu\frac{\partial \nu}{\partial r}\right\}+\alpha_\nu\mu\left|\frac{\partial u}{\partial r}\right|,\quad \mu=\rho\nu,\quad \alpha_\nu=0.2, \tag{2}$$

$$\frac{\partial \rho u r}{\partial x}+\frac{\partial \rho w r}{\partial r}=0, \tag{3}$$

$$\frac{\partial \rho u^2}{\partial x}+\frac{1}{r}\frac{\partial \rho u w r}{\partial r}=\frac{1}{r}\frac{\partial}{\partial r}\left\{r\mu\frac{\partial u}{\partial r}\right\}, \tag{4}$$

$$\frac{\partial \rho u H}{\partial x}+\frac{1}{r}\frac{\partial \rho w r H}{\partial r}=\frac{1}{r}\frac{\partial}{\partial r}\left\{\frac{r\mu}{\mathrm{Pr}}\frac{\partial H}{\partial r}\right\}+\frac{1}{r}\frac{\partial}{\partial r}\left\{r\mu\left(1-\frac{1}{\mathrm{Pr}}\right)u\frac{\partial u}{\partial r}\right\}, \tag{5}$$

$$H=C_pT+\frac{u^2+w^2}{2},$$

$$\frac{\partial \rho u Y}{\partial x}+\frac{1}{r}\frac{\partial \rho w r Y}{\partial r}=\frac{1}{r}\frac{\partial}{\partial r}\left\{\frac{r\mu}{\mathrm{Sc}}\frac{\partial Y}{\partial r}\right\},\quad Y=\frac{\rho_\nu}{\rho},\quad \mathrm{Sc}=\frac{\mu}{\rho D},\quad \mathrm{Pr}=\frac{C_p\mu}{k}. \tag{6}$$

The initial and boundary conditions have the following form:

at $x = 0$

$$0\le r<r_{a1}:\ u=u_{a1},\ w=0,\ H=H_{a1}\equiv C_pT_{a1}+u_{a1}^2/2,\ \nu=0.001\nu_{a1},\ Y=Y_a; \tag{7}$$

$$\nu(0,r_{a1})=\nu_{a1}\equiv C_{1\nu}r_{a1}\left|u_{a1}-u_{a2}\right|,\ C_{1\nu}=0.014; \tag{8}$$

$$r_{a1}\le r<r_a:\ u=u_{a2},\ w=0,\ H=H_{a2}\equiv C_pT_{a2}+u_{a2}^2/2,\ \nu=0.001\nu_a,\ Y=Y_\infty; \tag{9}$$

$$\nu(0,r_a)=\nu_a\equiv C_{2\nu}r_a\left|u_{a2}-u_\infty\right|,\ C_{2\nu}=0.014; \tag{10}$$

$$r_a\le r\le r_m:\ u=u_\infty,\ w=0,\ H=H_\infty\equiv C_pT_\infty+u_\infty^2/2,\ \nu=0.001\nu_a,\ Y=Y_\infty; \tag{11}$$

at $0\le x\le x_m$

$$r=0:\ \frac{\partial \nu}{\partial r}=0,\ \frac{\partial u}{\partial r}=0,\ w=0,\ \frac{\partial H}{\partial r}=0,\ \frac{\partial Y}{\partial r}=0; \tag{12}$$

$$r=r_m:\ \nu=0.001\nu_a,\ u=u_\infty,\ w=0,\ H=H_\infty,\ Y=Y_\infty. \tag{13}$$

Here u_{a1} and T_{a1} are the velocity and temperature at the edge of the nozzle in the inner duct of radius r_{a1} and u_{a2} and T_{a2} are the velocity and temperature in the outer duct of radius r_a. We relate the density ρ, velocity components u and w, and enthalpy H to the parameters in the co-current flow ρ_∞, u_∞, and H_∞, the coordinates x and r to r_a, and the coefficients of turbulent dynamic viscosity μ, thermal conductivity k, and diffusion D to the characteristic values $\mu_a = \rho_\infty\nu_a$, $k_a = C_p\mu_a/\mathrm{Pr}$, and $D_a = \nu_a/\mathrm{Sc}$. Not introducing special notation for dimensionless quantities, we obtain

$$p\approx 1,\quad \rho=1/T, \tag{14}$$

$$\rho u\frac{\partial \nu}{\partial x}+\rho w\frac{\partial \nu}{\partial r}=\frac{2}{r\,\mathrm{Re}}\frac{\partial}{\partial r}\left\{r\mu\frac{\partial \nu}{\partial r}\right\}+\alpha_\nu\mu\left|\frac{\partial u}{\partial r}\right|,\quad \mu=\rho\nu,\quad \mathrm{Re}=\frac{1}{C_{2\nu}\left|s_2-1\right|},\tag{15}$$

$$\frac{\partial \rho u r}{\partial x}+\frac{\partial \rho w r}{\partial r}=0,\tag{16}$$

$$\frac{\partial \rho u^2}{\partial x}+\frac{1}{r}\frac{\partial \rho u w r}{\partial r}=\frac{1}{r\,\mathrm{Re}}\frac{\partial}{\partial r}\left\{r\mu\frac{\partial u}{\partial r}\right\},\tag{17}$$

$$\frac{\partial \rho u H}{\partial x}+\frac{1}{r}\frac{\partial \rho w r H}{\partial r}=\frac{1}{r}\frac{\partial}{\partial r}\left\{\frac{r\mu}{\mathrm{Pe}}\frac{\partial H}{\partial r}\right\}+\frac{1}{r\left[1+\dfrac{2}{(\gamma-1)\,\mathrm{M}_\infty^2}\right]}\frac{\partial}{\partial r}\left\{\left(1-\frac{1}{\mathrm{Pr}}\right)\frac{r\mu}{\mathrm{Re}}\frac{\partial u^2}{\partial r}\right\},\tag{18}$$

$$\mathrm{Pe}=\mathrm{Re}\,\mathrm{Pr},\quad \gamma=\frac{C_p}{C_\nu},\quad M_\infty^2=\frac{u_\infty^2}{\gamma p_\infty/\rho_\infty},$$

$$\frac{\partial \rho u Y}{\partial x}+\frac{1}{r}\frac{\partial \rho w r Y}{\partial r}=\frac{1}{r}\frac{\partial}{\partial r}\left\{\frac{r\mu}{\mathrm{Re}\,\mathrm{Sc}}\frac{\partial Y}{\partial r}\right\}.\tag{19}$$

The initial and boundary conditions take on the following form:

at $x = 0$

$$0\le r<r_{a1}:\ u=s_1,\ w=0,\ H=h_1\equiv H_{a1}/H_\infty,\ \nu\approx 0.001,\ Y=Y_a,\tag{20}$$

$$\nu\,(0,r_{a1})=r_{a1}\frac{C_{1\nu}\left|s_1-s_2\right|}{C_{2\nu}\left|s_2-1\right|};\tag{21}$$

$$r_{a1}\le r<1:\ u=s_2,\ w=0,\ H=h_2\equiv H_{a2}/H_\infty,\ \nu=0.001,\ Y=Y_\infty,\tag{22}$$

$$\nu\,(0,1)=1;\tag{23}$$

at $0\le x\le x_m$

$$r=0:\ \frac{\partial \nu}{\partial r}=0,\ \frac{\partial u}{\partial r}=0,\ w=0,\ \frac{\partial H}{\partial r}=0,\ \frac{\partial Y}{\partial r}=0;\tag{24}$$

$$r=r_m:\ \nu=0.001,\ u=1,\ w=0,\ H=1,\ Y=Y_\infty\tag{25}$$

Turbulent Pr and Sc numbers are usually close to unity. We take Pr = Sc = 1. The co-currencies of the inner flow $1/s_1 = u_\infty/u_{a1}$ and the outer flow $1/s_2 = u_\infty/u_{a2}$, the parameters of heating $h_1 = H_{a1}/H_\infty$ and $h_2 = H_{a2}/H_\infty$, the relative mass concentration of vapor at the edge of the nozzle Y_a and in the atmosphere Y_∞, and the constants α_ν and $C_{1\nu}$ and $C_{2\nu}$ are the similarity parameters. The Reynolds number $\mathrm{Re} = u_\infty r_a/\nu_a$ is expressed in terms of the co-currency $1/s_2 = u_\infty/u_{a2}$ of the outer duct and in terms of $C_{2\nu}$. To solve the problem numerically, we used the implicit-difference scheme [17–19] of second order of approximation.

A Limiting Case of Uniform Transverse Distribution of the Coefficient of Viscosity for a Jet Equivalent in the Mass Flow Rate and Energy of Gas. We take typical initial values for the exhaust jet of a double-flow en-

gine: the cruise regime of flight at a height of 11 km, pressure p_∞ = 22,690 N/m^2, temperature of the standard atmosphere T_∞ = 216.7 K, velocity of flight u_∞ = 235.9 m/sec, radius of the inner duct r_{a1} = 0.333 m, velocity of exhaust gas u_{a1} = 388.2 m/sec, T_{a1} = 574.9 K, s_1 = 1.645, h_1 = 2.659, relative mass concentration of vapor Y_{a1} = 0.002288, partial density of vapor $\rho_{v,a1}$ = 0.00315 kg/m^3, radius of the outer duct r_{a2} = 0.869 m, velocity of exhaust gas u_{a2} = 322.8 m/sec, T_{a2} = 219.2 K, s_2 = 1.368, h_2 = 1.111, and $Y_{a2} = Y_\infty = S_\infty Y_{s,i\infty}$, where S_∞ is the relative humidity and $Y_{s,i\infty} = 4.58 \cdot 10^{-5}$ is the concentration of saturated vapor above ice at the temperature of the atmosphere.

The profiles of velocity, temperature, and other parameters in the initial cross section (7)–(13) differ from the uniform ones which are usually specified in the case of single-flow engines and even of double-flow engines with mixing. For a jet of radius r_a = 0.869 m, which is equivalent in flow rate of energy and mass of mixture and vapor, with uniform transverse distribution of all parameters (complete mixing of flows of the inner and outer ducts of the engine) we obtain

$$\pi r_a^2 \rho_a u_a = C_1 = \int_0^{r_a} 2\pi r \rho(r)\, u(r)\, dr \equiv \pi \left[r_{a1}^2 \rho_{a1} u_{a1} + (r_a^2 - r_{a1}^2) \rho_{a2} u_{a2} \right], \tag{26}$$

$$\pi r_a^2 \rho_a u_a (C_p T_a + u_a^2/2) = C_2 = \int_0^{r_a} 2\pi r \rho(r)\, u(r) \left[C_p T(r) + u^2(r)/2 \right] dr =$$

$$= \pi \left\{ r_{a1}^2 \rho_{a1} u_{a1} H_{a1} + (r_a^2 - r_{a1}^2) \rho_{a2} u_{a2} H_{a2} \right\}, \tag{27}$$

$$\rho_a = \frac{C_1}{\pi r_a^2 u_a}, \quad T_a = \frac{p_\infty m}{R \rho_a}, \quad u_a = \frac{-B + \sqrt{B^2 + 2C_1 C_2}}{C_1}, \quad B = \frac{\pi r_a^2 C_p p_\infty m}{R}, \tag{28}$$

$$\pi r_a^2 \rho_{v,a} u_a = C_3 = \int_0^{r_a} 2\pi r \rho_v(r)\, u(r)\, dr = \pi r_{a1}^2 \rho_{v,a1} u_{a1}, \quad \rho_{v,a} = \rho_{v,a1} \frac{r_{a1}^2 u_{a1}}{r_a^2 u_a}. \tag{29}$$

Here the velocity u_a = 331.1 m/sec, temperature T_a = 244.2 K, mixture density ρ_a = 0.324 kg/m^3, similarity parameters s = 1.403 and h = 1.222, relative mass concentration of vapor Y_a = 0.00168, and partial density of vapor $\rho_{v,a}$ = 0.00054 kg/m^3.

It is also possible to specify the coefficient of turbulent kinematic viscosity $\nu = \nu_{a1}$ and $\nu = \nu_a$ within a certain range of the transverse coordinate near the studied points (circumferences) rather than at the points $r = r_{a1}$ and $r = r_a$. For comparison sake we consider the limiting version where at $x = 0$ we have

$$0 \le r < r_{a1}: \quad \nu(0, r) = \nu_{a1} \equiv C_{1\nu} r_{a1} \left| u_{a1} - u_{a2} \right|, \tag{30}$$

$$r_{a1} \le r < r_a: \quad \nu(0, r) = \nu_a \equiv C_{2\nu} r_a \left| u_{a2} - u_\infty \right| \tag{31}$$

instead of (8) and (10).

Figure 1a shows the changes in the coefficient of kinematic viscosity $\nu(x, r = 0)$ along the x axis. The constants α_ν = 0.2 and $C_{1\nu} = C_{2\nu}$ = 0.014 constitute the *basic* version. The relative humidity of the atmosphere S_∞ = 0 (Y_∞ = 0). Figure 1b and c gives the transverse distribution of the coefficient of kinematic viscosity in the cross sections x = 60 m and $x \approx 150$ m. Noticeable differences between versions (8), (10) and (30), (31) are observed only up to the cross section with a maximum $\nu(x = x_{m\nu}, r = 0) = \max$ and behind this cross section within the range $\Delta x \sim x_{m\nu}$, whereas these differences are virtually absent for $x \ge 200$ m. The differences between the basic version and the jet, which is equivalent in mass flow rate and energy, of a single-flow engine are the following: in the second

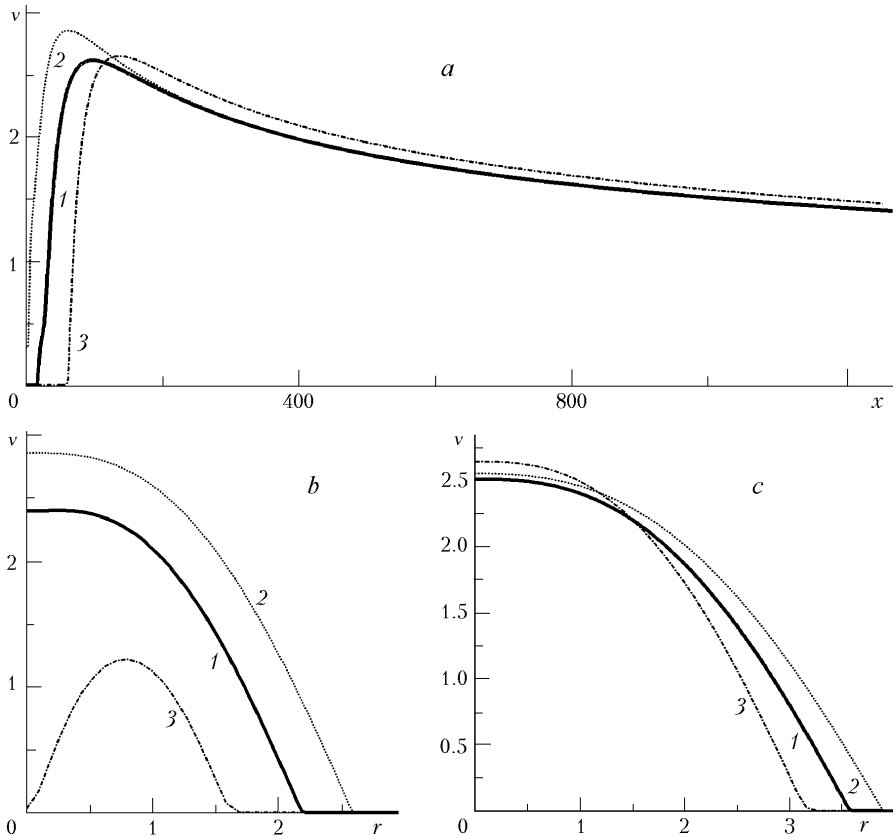

Fig. 1. Dependences of the coefficient of kinematic viscosity ν on the coordinate x along the jet axis (a); transverse distributions of ν (x = 60 m, r) (b) and ν (x = 150 m, r) (c) [1) initial velocity is assigned along the radius of the ducts according to (8), (10); 2) limiting case of disturbances in the entire initial cross section (30), (31); 3) jet of the single-flow engine, which is equivalent in flow rate of mass and energy], ν, m^2/sec; r, x, m.

case, the point (coordinate) of the maximum and the point of arrival of disturbances at the axis are displaced from the nozzle and the value of the coefficient of kinematic viscosity after reaching the maximum is somewhat higher.

For velocity and temperature, the length of the initial section with constant values of u and T decreases 5–10-fold for the limiting case (30), (31) and increases by about four times in the case of the equivalent jet (from the single-flow engine). The differences in the transverse distributions exceed 10% in the cross section x = 60 m and amount to only several percent when $x \approx 150$ m.

Figure 2 shows the changes in the concentration of vapor Y (curves 1–3) and ice $Y_i = \rho_i/\rho$ (curves 4–6) along and transverse to the jet. In the far field, the effect of the initial distribution of viscosity on small "admixtures" (components) of the exhaust gas mixture is more substantial than on temperature, velocity, and the coefficient of viscosity. This conclusion also refers to both the values on the axis and transverse distributions. Figure 3 presents the values of the jet cross-section mean concentration of vapor Y_{av} and condensate (ice) $Y_{i,av}$ along the jet:

$$Y_{av} = Y_\infty + Y_{1av}, \quad Y_{1av}(x) = \frac{\int_0^\infty 2\pi r\,[Y(x,r) - Y_\infty]\,dr}{\pi r_j^2}, \quad Y_{i,av}(x) = \frac{\int_0^{r_c} 2\pi r\,[Y(x,r) - Y_{s,i}]\,dr}{\pi r_c^2}. \tag{32}$$

Here r_j is the jet radius calculated by 1% of the velocity maximum on the axis. Up to the section of aerosol merging on the axis the radius of the condensation wake r_c is the outer boundary of condensation (crystallization) of the aerosol.

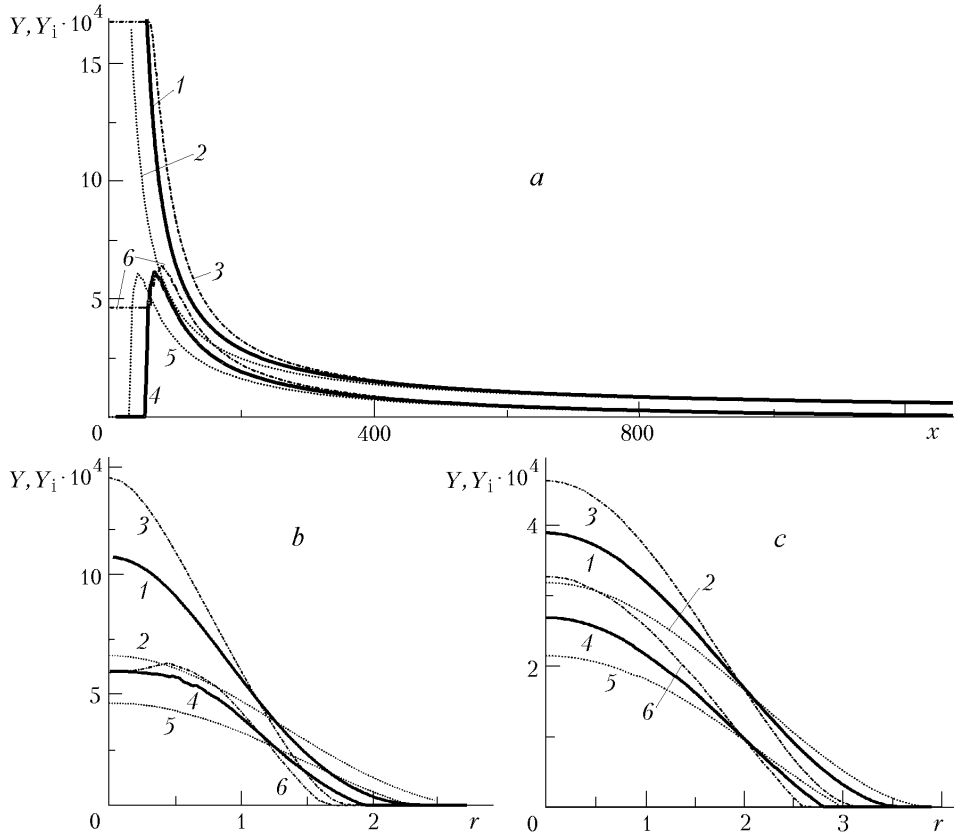

Fig. 2. Dependences of the concentrations of vapor Y (curves 1–3) and ice Y_i (curves 4–6) on the coordinate x along the jet axis (a) and their profiles at x = 70 m (b) and x = 150 m (c): 1 and 4) base, assignment of initial eddy viscosity at a point (on the circumference); 2 and 5) within the entire duct; 3 and 6) jet of the single-flow engine, which is equivalent in flow rate of mass and energy. r, x, m.

TABLE 1. Characteristic Cross Sections of the Exhaust Jet (m)

Line No.*)	x_*	$x_{m,i}$	x_m	$x_{m\nu}$	L_m
1	54.4	68.4	57.9	96.5	1269.4
2	30.96	42.9	33.3	60.5	1444.6
3	0	78.5	28.5	135	1255

*)Line 1 — $\nu(x = 0, r)$ according to (8), (10); line 2 — according to (30), (31); line 3 — jet of the single-flow engine, which is equivalent in flow rate of mass and energy.

The concentration of the vapor saturated above the condensate (in this case, ice) $Y_{s,i}$ is calculated by the Clausius–Clapeyron formula:

$$Y_{s,i}(T) = Y_{s,i\infty} \exp\left\{\int_{T_\infty}^{T} \frac{m_w L dT}{RT^2}\right\}. \tag{33}$$

At a distance x_m the value of the section-mean concentration of the condensate is maximum. The distance x_m slightly exceeds the distance $x = x_*$ to the section of aerosol merging on the axis and is slightly smaller (in the scale of the length of the condensation wake L_m) than the distance $x_{m,i}$ to the section of the maximum concentration of ice on the axis Y_i ($x = x_{m,i}$, $r = 0$) = max. At distances $x > x_*$ the transverse dimensions of the jet with respect to

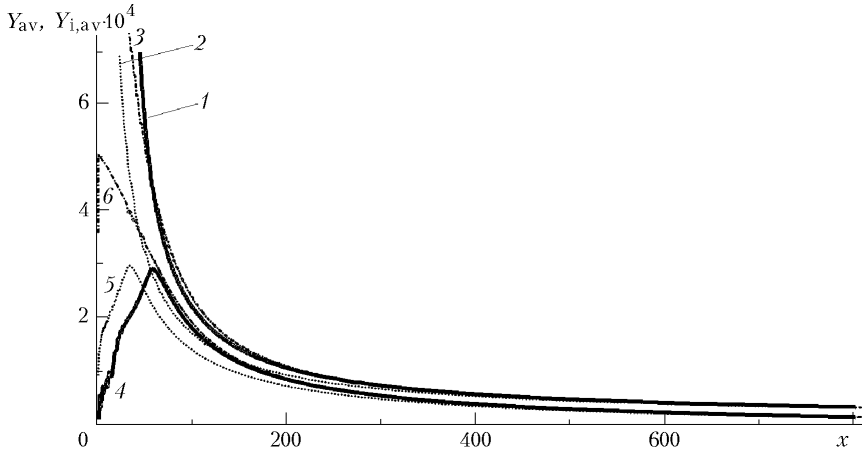

Fig. 3. Dependences of the mean concentration of vapor Y_{av} (curves 1–3) and condensate (ice) $Y_{i,av}$ (curves 4–6) on the distance x along the jet axis. For the notation of 1–6, see Fig. 2.

the velocity, temperature, and concentration of vapor coincide, as a rule. Values of x_*, $x_{m,i}$, x_m, $x_{m\nu}$, and L_m for the versions considered are given in Table 1. An analysis of the results presented in Table 1 allows one to draw the following conclusions.

The version of a narrow boundary layer of an infinitely small thickness (8), (10) and the limiting version of a turbulent flow within the entire cross section of both ducts of the nozzle (30), (31) differ; viz., in the second case, the maximum of the coefficient of kinematic viscosity is closer to the nozzle (Fig. 1a); near the nozzle, the profile ν (x = const, r) becomes dome-like (Fig. 1b and c); and the transition section of a sharp decrease in the temperature, velocity, and concentration of vapor begins immediately behind the edge of the nozzle (Fig. 2). The coordinates x_*, $x_{m,i}$, x_m, and $x_{m\nu}$ change greatly (~40%) and the length of the contrail L_m changes slightly (~14%). When $x \geq 200$ m, all parameters of these versions are virtually the same.

The version of a jet, which is equivalent in mass flow rate and energy, with uniform transverse distribution of all parameters across the edge of the nozzle (in complete mixing in a single-flow engine) differs from the basic version ($C_{1\nu} = 0.014 = C_{2\nu}$, $\alpha_\nu = 0.2$) with infinitely thin boundary layers in both ducts by a larger distance of the maximum of the coefficient of viscosity $\nu_m = \nu(x_{m\nu}, r = 0)$ from the nozzle. The coordinates of aerosol merging on the axis x_*, the maximum of the condensate concentration $x_{m,i}$, and section-mean concentration x_m are higher in the equivalent jet. The values of x_*, $x_{m,i}$, x_m, and $x_{m\nu}$ change by 100, 15, 51, and 40%, respectively; the length of the contrail L_m changes by 1.1%. Differences are negligibly small when $x \geq 300$ m.

Having studied the effect of transverse distribution of the coefficient of turbulence and having made a comparison with a single-flow engine, which is equivalent in mass flow rate and energy, we pass to the main objective of the study, i.e., we consider considerable changes (increase) of the coefficient of eddy viscosity in the initial cross section in order to execute monitoring of jet parameters in the far field.

Influence of Turbulence Enhancement on the Jet. By positioning notches or protrusions (pins) [which are commensurable with the thickness of the boundary laminar sublayer or the thickness of a turbulent layer on the nozzle walls (inner or outer, in the inner or outer ducts)] symmetrically around the circumference of the inner or outer ducts, we can substantially enhance the turbulence of the jet, increase the coefficient of viscosity at the edge of the nozzle, and, probably, to a lesser extent, increase the intensity of volumetric sources of eddy viscosity. In this case, the losses of thrust can be slight. In the physico-mathematical formulation of problem (1)–(13) this procedure means an increase of the constants $C_{1\nu}$, $C_{2\nu}$, and α_ν in the equation and boundary conditions in calculation of the coefficient of turbulent kinematic viscosity ν. Earlier it was suggested to increase smearing of the jet in a similar way [20, 21]. Of course, there is no complete analogy, in particular, due to the small dimensions of the pins in our case, which is important for preserving the flow rate of gas, fuel, and thrust.

We denote the *basic* variant with initial conditions (8), (10) for the coefficient of kinematic viscosity ν with constant $C_{1\nu} = 0.014 = C_{2\nu}$ and $\alpha_\nu = 0.2$ as I. We consider several variants of increase of eddy viscosity: variant II

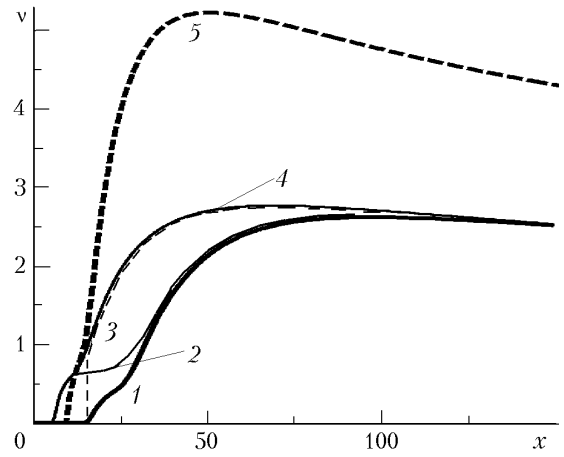

Fig. 4. Coefficient of turbulent kinematic viscosity ν along the x axis: 1) variant I; 2) II; 3) III; 4) IV; 5) V. ν, m^2/sec; x, m.

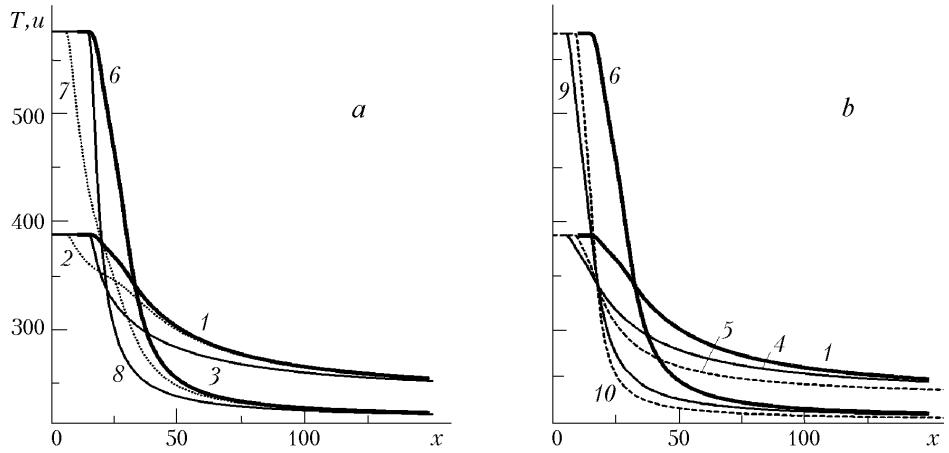

Fig. 5. Dependences of temperature T (curves 1–5) and velocity u (curves 6–10) on the distance x for variants I (1 and 6), II (2 and 7), and III (3 and 8) — a; I (1 and 6); IV (4 and 9), and V (5 and 10) — b. T, K; u, m/sec; x, m.

— $C_{1\nu} = 0.14$, $C_{2\nu} = 0.014$, and $\alpha_\nu = 0.2$; variant III — $C_{1\nu} = 0.014$, $C_{2\nu} = 0.14$, and $\alpha_\nu = 0.2$; variant IV — $C_{1\nu} = C_{2\nu} = 0.14$ and $\alpha_\nu = 0.2$; and variant V — $C_{1\nu} = 0.014$, $C_{2\nu} = 0.014$, and $\alpha_\nu = 0.4$.

Figure 4 shows the dependences of the coefficient of turbulent kinematic viscosity $\nu(x, r = 0)$ on distance x along the jet axis for variant II with the constant $C_{1\nu} = 0.14$ (increased by an order of magnitude) ($C_{2\nu} = 0.014$ and $\alpha_\nu = 0.2$, curve 2); for variant III with the constant $C_{2\nu} = 0.14$ (increased by an order of magnitude) ($C_{1\nu} = 0.014$ and $\alpha_\nu = 0.2$, curve 3); for variant IV with simultaneous increase of turbulence in both ducts (curve 4), and variant V with increase in the rate of turbulence generation in the jet volume (curve 5).

Figure 5 presents the dependences of temperature T (curves 1–5) and velocity u (curves 6–10) on distance x; Fig. 6 gives the dependences of the concentration of vapor Y (curves 1–5) and ice Y_i (curves 6–10) within the range $0 \le x \le 150$ m for variants I–V. When $x > 300$, the differences are less substantial, as well as for viscosity, temperature, and velocity.

An increase of turbulence in the first, closer to the axis, duct (variant II, Figs. 4, 5a, and 6a, curves 2 and 6) leads to a noticeable increase of viscosity near the edge of the nozzle. The transition section approaches the nozzle edge. The coordinates x_*, $x_{m,i}$, and x_m approach the nozzle. At a distance of $x > 50$ m the differences of the values of ν, T, u, and Y from the corresponding values of the basic variant I are already slight.

An increase in turbulence in the second duct (variant III, Figs. 4, 5a, and 6a, curves 3 and 7) marginally changes the length of the initial section with the parameters nondisturbed on the axis but leads to a stronger increase

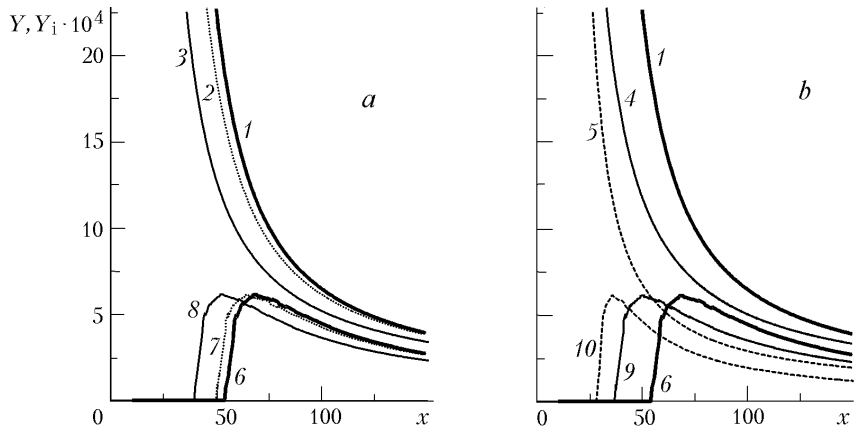

Fig. 6. Concentrations of vapor Y (curves 1–5) and ice Y_i (curves 6–10) along the x axis for variants I, II, and III (a) and I, IV, and V (b). For the notation of 1–10, see Fig. 5. x, m.

TABLE 2. Cross Sections of the Exhaust Jet x_*, $x_{m,i}$, x_m, $x_{m\nu}$, and L_m (m) for Variants I–V and the Corresponding Values of Contrail Radii: r_c^* and $r_{c,m}$ (m), Maxima of the Concentrations of Condensate (ice) on the Axis $Y_i(x_{m,i}, r = 0) = Y_{i,m}$ and Section-Mean $Y_{i,av}(x_m) = Y_{i,av,m}$ Maximum of the Coefficient of Kinematic Viscosity $\nu(x_{m\nu}) = \nu_m$ (m^2/sec)

No. of the variant	x_*/r_{c*}	$x_{m,i}/Y_{i,m}$	$x_m/Y_{i,av,m}$	$x_{m\nu}/\nu_m$	$L_m/r_{c,m}$
I	54.4/1.627	68.4/6.14e–4	57.9/2.89e–4	96.5/2.619	1269.4/1.967
II	49.7/1.609	64.4/6.14e–4	53.9/2.91e–4	94.3/2.636	1238/2.09
III	40.0/1.641	52.4/6.15e–4	43.7/2.89e–4	70.5/2.747	1211/2.09
IV	36.7/1.613	50.0/6.13e–4	41.3/2.89e–4	68.9/2.765	1208.9/2.075
V	28.8/1.629	36.0/6.13e–4	30.7/2.89e–4	50.5/5.222	685.0/2.171

of the coefficient of eddy viscosity; pronounced differences of all quantities from the basic variant are observed at distances of $x > 100$ m. The coefficients $C_{1\nu}$ and $C_{2\nu}$ in variants I and II are increased by an order of magnitude.

An increase in the coefficient of volumetric sources of turbulence α_ν only by a factor of two (variant V, Figs. 4, 5b, and 6b, curves 5 and 10) leads to a greater effect than simultaneous increase of the coefficients $C_{1\nu}$ and $C_{2\nu}$ by an order of magnitude (variant IV, Figs. 4, 5b, and 6b, curves 4 and 9).

Table 2 presents the main parameters of the jet for variants I–V. Maximum values of the concentration of condensate on the axis are $Y_{i,m} \approx 6.1 \cdot 10^{-4}$, section-mean values are $Y_{i,av,m} \approx 2.9 \cdot 10^{-4}$; they weakly change from variant to variant. This means that the optical thickness does not change greatly as well. The contrail radius is $r_c^* \approx 1.6$ m in the cross section x_*, and $r_{c,m} \approx 2$ m at its end cut off by an amount equal to 1% of the ratio between the condensate density ρ_i and its maximum value $\rho_{i,m}$ in order not to overestimate the length of the closing part, which virtually does not contribute to the total mass of the condensate. The maximum value of the condensate density $\rho_{i,m}$ usually lies on the axis near the cross section $x_{m,i}$.

With an increase of turbulence in the inner duct (increase of the constant $C_{1\nu}$ by an order of magnitude — variant II) the coordinates x_*, $x_{m,i}$, x_m, and $x_{m\nu}$ change by 8.6, 5.8, 6.9, and 2.3%, respectively; the contrail length L_m changes by 2.5%. An increase of turbulence in the outer duct (increase of $C_{2\nu}$ by an order of magnitude — variant III) leads to a stronger growth of the coefficient of eddy viscosity. The values of x_*, $x_{m,i}$, x_m, and $x_{m\nu}$ change by 26.5, 23.4, 24.5, and 27%, respectively; the contrail length L_m changes by 4.6%.

Simultaneous increase of the constants $C_{1\nu}$ and $C_{2\nu}$ by an order of magnitude (variant IV — $C_{1\nu} = 0.14 = C_{2\nu}$) leads to a change of the values of x_*, $x_{m,i}$, x_m, and $x_{m\nu}$ by 32.5, 26.9, 16.6, and 28.6%, respectively; the contrail length L_m changes by 4.8%. A twofold increase of the coefficient of volumetric sources of turbulence α_ν (variant V — $\alpha_\nu = 0.4$) results in a higher effect than simultaneous increase of the coefficients $C_{1\nu}$ and $C_{2\nu}$ by an order of magnitude. The coordinates x_*, $x_{m,i}$, x_m, and $x_{m\nu}$ change by 47, 47.4, 47, and 47.7%, respectively; the contrail length L_m changes by 46%.

The contrail length virtually does not change with an increase of turbulence only in the initial cross section $x = 0$ (with increase of the constants $C_{1\nu}$ and $C_{2\nu}$ only) by an order of magnitude and decreases two times with a two-fold increase in the intensity of turbulence generation in the jet volume (with an increase of the coefficient α_ν). In fact, α_ν will increase simultaneously with $C_{1\nu}$ and $C_{2\nu}$ if the turbulizers mentioned are used at the edge of the nozzle of the inner or outer ducts. The distances x_*, $x_{m,i}$, x_m, and $x_{m\nu}$ decrease to about two times with the considered increase of the parameters α_ν, $C_{1\nu}$, and $C_{2\nu}$.

An analysis of isolines of the concentration of condensate $Y_i = 0.8, 0.6, 0.4, 0.2\ Y_{i,m}$ for variants I–V shows that as the jet turbulence increases, the maximum of the condensate concentration and the contours of equal concentration gradually approach the edge of the nozzle. The hot core where condensation is absent decreases in size.

CONCLUSIONS

1. The effect of the initial transverse distribution of the coefficient of kinematic viscosity on the parameters of a turbulent exhaust jet is shown.

2. The presence of two ducts instead of one, which is equivalent in flow rate of mass and energy of gas, with infinitely thin boundary layers leads to a considerable change of the parameters of a turbulent exhaust jet.

3. An increase of turbulence in the inner duct (variant II) causes an increase of viscosity in the near field of the jet. The coordinates x_*, $x_{m,i}$, x_m, and $x_{m\nu}$ change up to 9%. An increase of turbulence in the outer duct (variant III) leads to substantial increase of the coefficient of eddy viscosity. Values of x_*, $x_{m,i}$, x_m, and $x_{m\nu}$ change up to 27%.

4. A simultaneous increase of the constants $C_{1\nu}$ and $C_{2\nu}$ by an order of magnitude (variant IV) results in a change of the values x_*, $x_{m,i}$, x_m, and $x_{m\nu}$ up to 33%, and an increase of the coefficient of volumetric sources of turbulence α_ν to about two times (variant V) leads to a larger effect. The coordinates x_*, $x_{m,i}$, x_m, and $x_{m\nu}$ change up to 48%.

5. The length of the condensation wake in variants II, III, and IV changes slightly; in variant V it decreases to about 50%.

6. The transverse geometric dimensions, concentration of the condensate, and maximum values of the kinematic coefficient of eddy viscosity in the considered variants I–V change slightly.

The author expresses his gratitude to V. K. Petrov for discussion of possible variants of initial parameters of the jet behind the double-flow engine and to M. N. Kogan for discussion of the results.

This work was supported by NASA grant No. NCC-1.

NOTATION

x and r, longitudinal and transverse coordinates; u and w, velocity components; ρ, p, and T, density, pressure, and temperature of gas; ν and μ, coefficients of kinematic and dynamic eddy viscosity; m and m_w, molar mass of the gas mixture and water vapor; R, universal gas constant; L, specific heat of condensation; H, total enthalpy of gas; Y and Y_i, concentrations of vapor and condensate (ice); Sc, Pr, Re, and Pe, Schmidt, Prandtl, Reynolds, and Peclet numbers; γ, adiabatic index; M, Mach number; D and k, coefficients of diffusion and thermal conductivity; C_p, heat capacity at constant pressure; α_ν, $C_{1\nu}$, and $C_{2\nu}$, numerical coefficients; r_{1a} and $r_{2a} = r_a$, radii of the inner and outer ducts of the nozzle; $1/s_1$ and $1/s_2$, parameters of co-currency of the inner and outer flows; h_1 and h_2, parameters of heating; S_∞, relative humidity of the atmosphere; $Y_{s,i\infty}$, concentration of vapor saturated above ice; r_j, jet radius; r_c, radius of the condensation wake; x_*, distance to the cross section of aerosol merging on the axis; x_m, cross section where the value of section-mean concentration of the condensate is maximum; L_m, length of the condensation wake; $x_{m,i}$, cross section of the maximum concentration of ice on the axis Y_i; $x_{m\nu}$, cross section of the maximum coefficient of viscosity. Indices: a, parameters at the edge of the nozzle at $x = 0$; av, mean parameters when $x > 0$; c, condensation wake; i, ice; j, jet; v, vapor; s, saturated; w, water; ∞, at a large distance in nondisturbed gas; m, maximum; 1 and 2, inner and outer ducts, mν, maximum of viscosity.

REFERENCES

1. *Proc. Int. Colloq. "Impact of Aircraft Emissions upon the Atmosphere"*, 15–18 October 1996, Paris, Vol. I, pp. 1–378; Vol. II, pp. 379–667 (1996).
2. U. Schumann (ed.), *Pollutants from Air Traffic* (*Results of Atmospheric Research in 1992–1997), German Aerospace Center, Oberpfafenhofen (1997).*
3. O. B. Popovicheva, A. M. Starik, and O. N. Favorskii, Problems of the effect of aviation on gas and aerosol composition of the atmosphere, *Izv. Ross. Akad. Nauk, Fiz. Atmos. Okeana*, **36**, No. 2, 163–176 (2000).
4. A. N. Kucherov, Blooming channel in contrails, *Opt. Atmos. Okeana*, **13**, No. 5, 521–528 (2000).
5. L. S. G. Kovasznay, Structure of the turbulent boundary layer, *Phys. Fluids*, **10**, No. 9, Pt. 2, 25–30 (1967).
6. V. M. Nee and L. S. G. Kovasznay, Simple phenomenological theory of turbulent shear flows, *Phys. Fluids*, **12**, No. 3, 473–484 (1969).
7. A. N. Sekundov, Application of the differential equation for eddy viscosity to the analysis of plane non-self-similar flows, *Izv. Akad. Nauk SSSR, Mekh. Zhidk. Gaza*, No. 5, 114–127 (1971).
8. V. I. Kopchenov, Method of numerical solution of the problem on propagation of a supersonic underexpanded turbulent jet in a co-current supersonic flow, *Uch. Zap. TsAGI*, **11**, No. 4, 37–44 (1980).
9. N. F. Borisov, Numerical calculation of nonisobaric supersonic viscous jets issuing into co-current supersonic flows, *Uch. Zap. TsAGI*, **16**, No. 1, 15–26 (1985).
10. P. Bradshaw, B. E. Launder, and J. Lumley, Collaborative Testing of Turbulence Models, AIAA Paper No. 91-0215 (1991).
11. A. N. Gulyaev, V. E. Kozlov, and A. N. Sekundov, Development of a universal one-parameter model for eddy viscosity, *Izv. Ross. Akad. Nauk, Mekh. Zhidk. Gaza*, No. 4, 69–81 (1993).
12. G. N. Abramovich, T. A. Girshovich, S. Yu. Krasheninnikov, et al., *Theory of Turbulent Jets* [in Russian], Nauka, Moscow (1984).
13. A. N. Kucherov, A. P. Markelov, A. A. Semenov, and A. V. Shustov, Initial contrail parameters dependence on flight conditions and parameters of exhaust gas, in: *Proc. Vth Int. Symp. "New Aviation Technology of the XXI Century*," 17–22 August 1999, Zhukovsky, Russia, Section 1.1 (1999), pp. 382–389.
14. A. N. Kucherov and G. V. Molleson, Condensation wake in a nonisobaric jet, *Inzh.-Fiz. Zh*., **74**, No. 5, 29–32 (2001).
15. A. V. Kashevarov and A. N. Kucherov, Strong effect of the shape of distributions of the parameters at the edge of the nozzle on the characteristics of the condensation wake, *Uch. Zap. TsAGI*, **33**, Nos. 1–2, 100–110 (2002).
16. A. V. Kashevarov, A. N. Kucherov, and G. V. Molleson, Dependence of optical characteristics of the condensation wake on the laws of distribution of parameters of a nonisobaric exhaust at the edge of the nozzle, *Opt. Atmos. Okeana*, **14**, No. 5, 418–423 (2001).
17. V. A. Ruskol and U. G. Pirumov, Isobaric turbulent reacting jet issuing into the co-current flow, *Dokl. Akad. Nauk SSSR*, **236**, No. 2, 321–324 (1977).
18. V. S. Avduevskii, D. A. Ashratov, A. V. Ivanov, and U. G. Pirumov, *Supersonic Nonisobaric Gas Jets* [in Russian], Mashinostroenie, Moscow (1985).
19. V. S. Avduevskii, D. A. Ashratov, A. V. Ivanov, and U. G. Pirumov, Gas Dynamics of Supersonic Nonisobaric Jets [in Russian], Mashinostroenie, Moscow (1989).
20. S. S. Pannu and N. H. Johannesen, Structure of jets from notched nozzles, *J. Fluid Mech.*, **74**, Pt. 3, 515–528 (1976).
21. Yu. G. Zhulev, N. T. Mallabaev, and A. G. Nalivaiko, Study of the possibility of enhancing smearing of co-current jets, *Izv. Ross. Akad. Nauk, Mekh. Zhidk. Gaza*, No. 5, 182–190 (1998).